Use of the (p,γ) reaction on semi-thick targets in the spectroscopy of odd mass nuclei

T. Paradellis and G. Vourvopoulos
Tandem Accelerator Laboratory, Nuclear Research Center "Democritos," Aghia Paraskevi, Athens, Greece

G. Costa
Centre de Recherches Nucléaires et Université Louis Pasteur, Strasbourg, France

E. Sheldon
Department of Physics and Applied Physics, University of Lowell, Lowell, Massachusetts 01854
(Received 5 May 1980; revised manuscript received 30 March 1981)

Singles γ-ray angular distributions obtained from the (p,γ) reaction on ^{56}Fe, ^{62}Ni, ^{66}Zn, and ^{68}Zn targets having a thickness of 3–5 mg/cm^2 are used to evaluate the statistical tensors for the alignment of the low-lying levels of ^{57}Co, ^{63}Cu, ^{67}Ga, and ^{69}Ga. The results show that these levels acquire a relatively strong alignment which depends only on the spin of the low-lying state. This fact makes the method suitable for spectroscopic investigation of odd mass nuclei. It has also been found that the observed Doppler shift of the transition in these nuclei can yield information on the lifetimes of the excited states upon the assumption of a side feeding time of 20 fs for the continuum γ cascades. The method is illustrated with the examination of the level properties of the ^{69}Ga nucleus.

[NUCLEAR REACTIONS ^{56}Fe, ^{62}Ni, ^{66}Zn, ^{68}Zn (p,γ), $E=2.0$–4.0 MeV. Measured $I\gamma(\theta)$. ^{57}Co, ^{63}Cu, ^{67}Ga, ^{69}Ga deduced statistical tensors for alignment, side feeding time. ^{69}Ga levels deduced J, δ, τ. Enriched targets, Ge(Li) detectors.]

I. INTRODUCTION

Proton radiative-capture reactions have traditionally been used with success to obtain information on nuclear structure. Their investigation continues to provide a valuable means of gaining insight into details of nuclear spectroscopy, alignment, and transition characteristics. The combination of strong absorption and electromagnetic decay offers unique properties for nuclear reaction studies.

The experimental approach has typically employed targets having a thickness of a few keV. Such targets were subjected to proton bombardment at energies ranging from a few hundred keV to several MeV. Measurements of the resulting γ-ray yield as a function of incident proton energy give information on the existence and location of resonances in the compound nucleus. Under appropriate conditions, measurements of the angular distributions of the γ rays from the decay of a particular resonance can provide information on the spin (and, possibly, parity) of the resonance, the multipole character of the γ transition, and the spin of the final nuclear state. The degree of nuclear alignment can in principle be deduced from the anisotropy of the outgoing γ radiation.

Hitherto, the underlying techniques have almost exclusively been based on the use of very thin targets, in order to avoid exciting more than a single resonance at any one time and thereby cause the angular distribution pattern to be perturbed by interference effects. Any complications in the shape of the angular distribution would tend to obscure the incisiveness of the analysis and hamper or confuse the interpretation. Indeed, it has become widely accepted that, for sufficiently thick targets and for sufficiently high level densities in the compound nuclei, the emergent γ radiation would evince zero, or negligibly small, anisotropy. This would render the method useless for nuclear spectroscopy.

A viable alternative to these two extremes exists, however, in the use of *semi*-thick targets i.e., targets through which the bombarding beam would lose 300 to 500 keV of energy, exciting thus a large number of states in the compound nucleus. Though largely neglected in the past, this constitutes a valuable compromise between either extreme and carries distinct advantages over either very thin or very thick target usage.

Recently, Nemashkalo *et al.*[1,2] have shown that when a semi-thick target is employed, and a sufficiently large number of compound nuclear levels are excited in the course of a radiative capture reaction, a γ-γ triple correlation may be analyzed in the framework of a statistical theory as a means of acquiring information on the low-lying levels of the residual nucleus. In this technique, a gate is placed on an NaI γ detector which registers photons originating from the excited levels that participated in transitions to the low-lying levels. The angular distributions of the γ rays deexciting the low-lying levels are recorded in a Ge(Li) de-

tector in coincidence with the NaI detector. From analyses of these data, when subjected to an appropriate correction and fitting procedure, conclusive spin assignments and multipolarity inferences may be drawn for the low-lying levels and the γ transitions.

In the present work, we show that semi-thick targets may be used along with singles γ-ray angular distributions (referred to the incident proton direction) to obtain detailed microscopic information on the low-lying levels of residual odd-mass nuclei. Specifically, we will show that in the cases investigated, where the target is an even-even nucleus having a thickness of a few mg/cm^2, the resulting alignment of the low-lying states in the residual nucleus is sufficiently strong to permit meaningful angular-distribution analyses to be performed and, moreover, that the resulting statistical tensors prove to be effectively constant over a range of bombarding energies and target atomic numbers, their only significant dependence being upon their spin. It will also be shown that the Doppler shift exhibited by the lower lying states in the residual nucleus can be analyzed in the frame of an effective side feeding time correction and thus allow the measurement of mean lives in the range of 20 to 500 fs.

From this study, a complete analogy is established between the (p,γ) reaction and other types of nuclear reaction processes, such as inelastic scattering, (p,p',γ) or $(p,n\gamma)$, or even $(a,n\gamma)$, in which statistical compound-nucleus model analyses are used[3] for the interpretation of experimental findings in nuclear structure, transition, and feeding studies.

II. EXPERIMENTAL METHOD AND RESULTS

A. General

The experiments were conducted at the Tandem Accelerator Laboratory, NRC Demokritos, using the 5 MV T11/25 Tandem Van de Graaff accelerator and at the CNRS-Strasbourg using the 3 MeV single-ended accelerator of the Laboratoire des Basses Energies. Self-supported targets with 99% enrichment in ^{56}Fe, ^{62}Ni, and ^{66,68}Zn were used in the measurements. In general, the targets had a thickness of 3 to 4 mg/cm^2 and were arranged at 45° with respect to the incident beam in a miniature aluminum or glass chamber.

Gamma ray spectra were recorded at several angles between 0° and 150° using Ge(Li) detectors with volumes in the range of 40–60 cm^3 and resolution ranging from 2.1 to 2.3 keV full width at half maximum (FWHM) at 1.3 MeV. The detectors were mounted on an angular distribution table and at various detector to target distances ranging from 7 to 15 cm, depending on the yield of the reaction.

The preamplifier pulse signals were routed to two amplifiers. The gain of the first amplifier was adjusted to record events up to 2.5 MeV, while the gain of the second amplifier was set to record events up to 12 MeV. A second Ge(Li) detector maintained at a fixed position served as a monitor.

The beam intensity during these experiments was kept low in order to prevent dead times exceeding 10%. The beam charge collected from the targets was used to trigger two pulse generators. The output signals of the pulse generators were fed to the inputs of the two Ge(Li) detectors used in the measurements, so that simultaneous dead time losses could be monitored.

Alignment of the detector-scattering chamber assembly was initially established via radioactive point sources and subsequently checked with the ^{27}Al (p,p',γ) reaction.

B. Angular distributions

Angular distributions of emitted γ rays from the residual nuclei ^{57}Co, ^{63}Cu, ^{67,69}Ga have been measured at several bombarding energies between 2 and 4 MeV. The experimental angular distributions were fitted by a least squares procedure to a Legendre polynomial expansion

$$W(\theta) = \sum_{\nu=0}^{\nu_{max}} Q_\nu A_\nu P_\nu(\cos\theta), \tag{1}$$

where Q_ν are the appropriate solid angle correction factors of the pertinent detectors. Initially, the data were fitted for all ν values up to $\nu = 4$. All the data indicated that the resulting odd order Legendre weighting coefficients A_ν were negligible within error, reflecting thus the symmetry of the angular distributions about 90°. Consequently, the data were fitted solely with even order Legendre polynomials with ν up to 4.

For a specific γ transition $J_i \xrightarrow{\delta} J_f$ involving multipolarity mixing ratio δ (defined here in terms of emission matrix elements[4]) the term A_ν in Eq. (1) may be written as

$$A_\nu(J_i, J_f;\ \delta) \equiv \rho_\nu(J_i) L_\nu(J_i, J_f;\ \delta), \tag{2}$$

where $\rho_\nu(J_i)$ is the Fano statistical tensor of the deexciting level J_i, and $L_\nu(J_i, J_f;\ \delta)$ is the γ-transition linking parameter made up of a weighted sum of Ferentz-Rosenzweig parameters,

$$L_\nu(J_i, J_f;\ \delta) = \frac{1}{1+\delta^2}\left[F_\nu(J_f L_i L_1 J_i) + 2\delta F_\nu(J_f L_1 L_2 J_i) + \delta^2 F_\nu(J_f L_2 L_2 J_i)\right]. \tag{3}$$

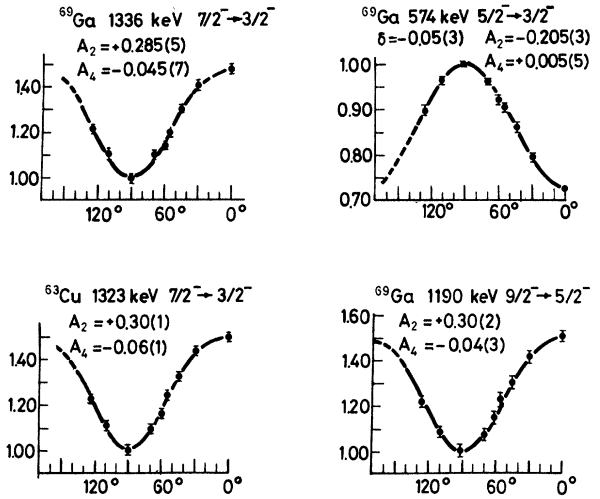

FIG. 1. Examples of some measured angular distributions.

For the present calculations the extensive tabulation of the functions F_ν of Yamazaki[5] has been used to calculate the expression $L_\nu(J_i, J_f; \delta)$ in all cases where J_i, J_f, and δ are known, in the residual nuclei ^{57}Co, ^{63}Cu, and ^{67,69}Ga. The statistical tensors $\rho_\nu(J_i)$ were then estimated by using the experimentally obtained weighting coefficients of the Legendre polynomial expansion A_ν in Eq. (2).

Since the value of L_ν [Eq. (3)] is very sensitive to the value of δ, only transitions between levels in the residual nuclei where the mixing ratio has been established by at least two separate experiments were used to extract statistical tensors. In a few cases involving low lying levels, an estimate was made also of the effect upon the statistical tensor $\rho_\nu(J)$ of the observed feeding by preceding transitions from higher lying levels. In Fig. 1 some angular distributions are shown together with the pertinent data used to extract the statistical tensors.

For all measured angular distributions, the data used from the literature and the deduced statistical tensors for ^{57}Co, ^{63}Cu, ^{67}Ga, and ^{69}Ga are listed in Tables I through IV for the experiments conducted at $E_p = 3$ MeV. For the cases of ^{67}Ga and ^{69}Ga the quoted experimental angular distributions are the average of two separate experiments conducted at the same bombarding energy.

From an inspection of these tables two conclusions can be drawn:

(i) The statistical tensors $\rho_\nu(J)$ remain constant within an average experimental error of 10% as a function of the excitation energy of the low lying level in the residual nucleus (at least up to $E^* = 2$ MeV), and appear to be only a function of the spin J of the level.

(ii) The tensor $\rho_\nu(J)$ for a given J value remains constant within better than 10% as a function of the atomic number Z, at least over the mass region studied here. In Table V the average deduced tensors $\rho_\nu(J)$ at the incident energy of 3 MeV as obtained from all available data are listed along with their statistical errors.

In practice, instead of the statistical tensor, the attenuation coefficient is often used:

$$\alpha_\nu \equiv \rho_\nu(J)/B_\nu(J), \tag{4}$$

where $B_\nu(J)$ is the statistical tensor for maximum alignment.[5] The corresponding $\alpha_\nu(J)$'s are also listed in Table V.

To examine the possible variation of the statis-

TABLE I. Summary of the data concerning the determination of the statistical tensor for $J = \frac{3}{2}$ at $E_p = 3$ MeV.

Nucleus	Level (keV)	$J_i^\pi \to J_f^\pi$	M	δ[a]	A_2[b]	$L_2(\delta)$[c]	ρ_2	A_4[b]	$L_4(\delta)^c\rho_4$
^{69}Ga	872	$\frac{3}{2}^- - \frac{3}{2}^-$	$E2/M1$	−0.12 (4)	0.041 (6)	−0.21 (6)	−0.20 (6)	0.005 (7)	
^{67}Ga	828	$\frac{3}{2}^- - \frac{3}{2}^-$	$E2/M1$	−0.16 (2)	0.047 (5)	−0.148 (31)	−0.32 (8)	0.010 (11)	
		$\frac{3}{2}^- - \frac{1}{2}^-$	$E2/M1$	−0.36 (9)	−0.24 (2)	0.937 (43)	−0.26 (3)	0.02 (2)	
	1640	$\frac{3}{2}^- - \frac{1}{2}^-$	$E2/M1$	−0.23 (7)	−0.22 (2)	0.828 (67)	−0.27 (3)	0.03 (2)	
^{63}Cu	1574	$\frac{3}{2}^- - \frac{3}{2}^-$	$E2/M1$	0.13 (4)	0.16 (2)	−0.591 (54)	−0.27 (4)	0.02 (3)	
^{57}Co	1378	$\frac{3}{2}^- - \frac{7}{2}^-$	$E2$	0	0.031 (3)	−0.143	−0.22 (2)	−0.01 (1)	
	1754	$\frac{3}{2}^- - \frac{7}{2}^-$	$E2$	0	0.032 (10)	−0.143	−0.22 (7)	0.02 (2)	

[a] Data for ^{69}Ga from Ref. 6, ^{67}Ga from Refs. 7 and 8, ^{63}Cu from Refs. 9 and 10, ^{57}Co from Refs. 11 and 12.
[b] As measured in this work.
[c] As defined in Eq. (3) in the text.

TABLE II. Summary of the data concerning the determination of the statistical tensor for $J=\frac{5}{2}$ at $E_p=3$ MeV.

Nucleus	Level (keV)	$J_i \to J_f$	M	δ[a]	A_2[b]	$L_2(\delta)$[c]	ρ_2	A_4[b]	$L_4(\delta)$[c]	ρ_4
^{69}Ga	574	$\frac{5}{2}^- - \frac{3}{2}^-$	$E2/M1$	−0.05 (3)	−0.210 (3)	0.467 (55)	−0.45 (5)	0.006 (5)	0.002 (2)	
	1725	$\frac{5}{2}^- - \frac{1}{2}^-$	$E2$	0	0.22 (4)	−0.535	−0.41 (8)	−0.06 (6)	−0.617	$\leqslant 0.195$
^{67}Ga	359	$\frac{5}{2}^- - \frac{3}{2}^-$	$E2/M1$	−0.07 (2)	−0.241 (5)	0.503 (36)	−0.48 (4)	0.003 (7)	0.003 (1)	
	911	$\frac{5}{2}^- - \frac{3}{2}^-$	$E2/M1$	0.33 (1)	0.10 (1)	−0.246 (17)	−0.41 (5)	0.010 (10)	0.069 (4)	0.15 ± 0.15
		$\frac{5}{2}^- - \frac{1}{2}^-$	$E2$	0	0.24 (8)	−0.535	−0.45 (15)	−0.06 (10)	−0.617 (18)	$\leqslant 0.26$
	1554	$\frac{5}{2}^- - \frac{3}{2}^-$	$E2/M1$	0.46 (4)	0.21 (2)	−0.445 (53)	−0.47 (7)	0.05 (4)	0.123 (18)	
		$\frac{5}{2}^- - \frac{5}{2}^-$	$E2/M1$	−0.58 (3)	−0.08 (2)	0.168 (23)	−0.48 (12)	0.02 (2)	−0.10 (1)	$\leqslant 0.4$
	2124	$\frac{5}{2}^- - \frac{3}{2}^-$	$E2/M1$	−0.27 (10)	−0.39 (8)	0.81 (13)	−0.48 (13)	0.04 (10)	0.05 (3)	
^{63}Cu	962	$\frac{5}{2}^- - \frac{3}{2}^-$	$E2/M1$	−0.48 (3)	−0.472 (5)	1.009 (16)	−0.47 (1)	0.000 (6)	0.132 (14)	0.00 (5)
	1412	$\frac{5}{2}^- - \frac{3}{2}^-$	$E2/M1$	0.61 (4)	0.31 (1)	−0.623 (38)	−0.50 (3)	0.01 (1)	0.191 (19)	0.05 (5)
	2082	$\frac{5}{2}^- - \frac{7}{2}^-$	$E2/M1$	0.28 (8)	−0.21 (6)	0.510 (90)	−0.41 (14)	0.01 (8)	0.01 (1)	
	2337	$\frac{5}{2}^- - \frac{7}{2}^-$	$E2/M1$	0.02 (2)	−0.16 (5)	0.336 (39)	−0.48 (15)	0.00 (7)	0.0	
^{57}Co	1919	$\frac{5}{2}^- - \frac{7}{2}^-$	$E2/M1$	−0.24 (3)	0.07 (2)	−0.171 (32)	−0.41 (14)	0.02 (3)	0.0	
	2133	$\frac{5}{2}^- - \frac{7}{2}^-$	$M1$	0.0 (4)	−0.06 (2)	0.134 (55)	−0.45 (30)	−0.02 (3)	0.0	

[a] Data for ^{69}Ga from Ref. 6, ^{67}Ga from Refs. 7 and 8, ^{63}Cu from Refs. 9 and 10, ^{57}Co from Refs. 11 and 12.
[b] As measured in this work.
[c] As defined in Eq. (3) in the text.

tical tensor as a function of the bombarding energy, the experiments have been repeated at $E_p = 2.0$, 2.9, 3.3, and 4 MeV. The resulting averaged data are listed in Table VI. Apart from an apparent slight increase in the case of $\rho_2(\frac{3}{2})$ when the proton energy increases from 2 to 3 MeV, the

TABLE III. Summary of the data concerning the determination of the statistical tensor of $J=\frac{7}{2}$ at $E_p=3$ MeV.

	Level (keV)	$J_i^\pi \to J_f^\pi$	M	δ[a]	A_2[b]	$L_2(\delta)$[c]	ρ_2	A_2[b]	$L_4(\delta)$[c]	ρ_4
^{69}Ga	1336	$\frac{7}{2}^- - \frac{3}{2}^-$	$E2$	0	0.295 (5)	−0.468	−0.63 (1)	−0.050 (10)	−0.358	0.14 (3)
	1448	$\frac{7}{2}^- - \frac{3}{2}^-$	$E2$	0	0.29 (2)	−0.468	−0.62 (4)	−0.07 (2)	−0.358	0.20 (6)
		$\frac{7}{2}^- - \frac{5}{2}^-$	$E2/M1$	−2.5 (1)	−0.36 (2)	0.630 (23)	−0.57 (5)	0.08 (2)	0.549 (6)	0.15 (1)
^{67}Ga	1202	$\frac{7}{2}^- - \frac{3}{2}^-$	$E2$	0	0.31 (1)	−0.468	−0.66 (2)	−0.08 (2)	−0.358	0.22 (6)
		$\frac{7}{2}^- - \frac{5}{2}^-$	$E2/M1$	−3.15 (5)	−0.32 (3)	0.504 (8)	−0.64 (6)	0.06 (3)	0.578 (2)	0.10 (5)
	1413	$\frac{7}{2}^- - \frac{3}{2}^-$	$E2$	0	0.31 (1)	−0.468	−0.66 (2)	−0.07 (1)	−0.358	0.20 (3)
		$\frac{7}{2}^- - \frac{5}{2}^-$	$E2/M1$	−1.42 (9)	−0.66 (3)	0.946 (31)	−0.70 (4)	0.09 (3)	0.43 (2)	0.21 (7)
^{63}Cu	1323	$\frac{7}{2}^- - \frac{3}{2}^-$	$E2$	0	0.30 (1)	−0.468	−0.64 (2)	−0.06 (1)	−0.358	0.17 (3)
	1863	$\frac{7}{2}^- - \frac{3}{2}^-$	$E2$	0	0.30 (2)	−0.468	−0.64 (2)	−0.06 (2)	−0.358	0.17 (3)
		$\frac{7}{2}^- - \frac{5}{2}^-$	$E2/M1$	0.05 (3)	−0.15 (2)	0.232 (58)	−0.65 (18)	0.01 (2)	0.002 (2)	
	2092	$\frac{7}{2}^- - \frac{5}{2}^-$	$E2/M1$	−1.06 (22)	−0.74 (5)	1.056 (64)	−0.70 (6)	0.05 (5)	0.337 (58)	0.15 (15)
	2404	$\frac{7}{2}^- - \frac{5}{2}^-$	$E2/M1$	−0.25 (4)	−0.48 (10)	0.748 (53)	−0.64 (14)	−0.02 (14)	0.037 (12)	
^{57}Co	1897	$\frac{7}{2}^- - \frac{9}{2}^-$	$E2/M1$	0.09 (6)	−0.22 (3)	+0.286 (92)	−0.77 (27)	−0.01 (4)	0.002 (2)	
	2311	$\frac{7}{2}^- - \frac{9}{2}^-$	$E2/M1$	0.09 (3)	−0.21 (3)	+0.286 (44)	−0.73 (10)	0.05 (4)	0.003 (3)	

[a] Data for ^{69}Ga from Ref. 6, ^{67}Ga from Refs. 7 and 8, ^{63}Cu from Refs. 9 and 10, ^{57}Co from Refs. 11 and 12.
[b] As measured in this work.
[c] As defined in Eq. (3) in the text.

TABLE IV. Summary of the data concerning the determination of the statistical tensor for $J=\frac{9}{2}$ at $E_p=3$ MeV.

	Level (keV)	$J_f^\pi - J_i^\pi$	M	δ[a]	A_2[b]	$L_2(\delta)$[c]	ρ_2	L_4[b]	$F_4(\delta)$[c]	ρ_4
^{69}Ga	1765	$\frac{9}{2}^- - \frac{5}{2}^-$	$E2$	0	0.31 (2)	−0.432	−0.72 (5)	−0.04 (2)	−0.268	0.15 (7)
	1972	$\frac{9}{2}^+ - \frac{7}{2}^-$	$E1$	0	−0.21 (2)	0.303	−0.69 (7)	0.01 (2)	0.0	
		$\frac{9}{2}^+ - \frac{7}{2}^-$	$E1$	0	−0.19 (2)	0.303	−0.63 (6)	−0.01 (2)	0.0	
^{67}Ga	1519	$\frac{9}{2}^- - \frac{5}{2}^-$	$E2$	0	0.33 (2)	−0.432	−0.76 (5)	−0.10 (3)	−0.268	0.37 (11)
	2074	$\frac{9}{2}^+ - \frac{7}{2}$	$E1$	0	−0.19 (3)	0.303	−0.63 (10)	0.04 (4)	0.0	
		$\frac{9}{2}^+ - \frac{9}{2}^-$	$E1$	0	0.31 (5)	−0.440	−0.71 (11)	0.00 (6)	0.0	
^{63}Cu	2208	$\frac{9}{2}^- - \frac{5}{2}^-$	$E2$	0	0.26 (6)	−0.432	−0.60 (14)	−0.11 (7)	−0.268	0.41 (26)
		$\frac{9}{2}^- - \frac{7}{2}^-$	$E2/M1$	−0.26 (2)	−0.57 (7)	0.738 (27)	−0.77 (10)	−0.02 (8)	0.0	
	1224	$\frac{9}{2}^- - \frac{7}{2}^-$	$E2/M1$	0.23 (1)	0.083 (10)	−0.122 (17)	−0.68 (12)	0.015 (13)	0.0	

[a] Data for ^{69}Ga from Ref. 6, ^{67}Ga from Refs. 7 and 8, ^{63}Cu from Refs. 9 and 10, ^{57}Co from Refs. 11 and 12.
[b] As measured in this work.
[c] As defined in Eq. (3) in the text.

remaining data show that the statistical tensors remain constant within better than 10%.

In order to ensure that no strong resonances dominate the decay pattern of the compound nucleus, continuous monitoring of the high energy γ-ray continuum was employed up to the end point energy. The continuum γ-ray spectra obtained at all measured angles in all reactions were also analyzed by slicing the spectra into 0.5 MeV steps and treating the bins so generated as individual peaks. The angular distribution of the continuum proved to be nearly isotropic. Actually, the average of 40 such measurements yielded

$$A_2 = -0.011\ (15)$$

and

$$A_4 = +0.001\ (20).$$

The essential conclusions of these observations are the apparent independence of the statistical tensor of the details of the deexcitation pattern of the compound nucleus, and its dependence on the spin of the observed level. This is exactly what makes the method a very useful spectroscopic tool. A knowledge of the statistical tensor as a function of spin can now be used along with the measured angular distributions of γ rays deexciting levels with otherwise unknown properties, to determine possible spin assignments (sometimes even unique) and mixing ratios in complete analogy with other types of compound mechanism reactions of the type (x,x',γ). In Sec. III, the results of such an investigation of the levels of ^{69}Ga up to 2.3 MeV excitation energy are given to allow for an evaluation of the usefulness of the method.

TABLE V. Overall data average of the statistical tensors at $E_p=3$ MeV and the corresponding attenuation coefficients of the alignment.[a]

J	$\rho_2(J)$	$\alpha_2(J)$	$\rho_4(J)$	$\alpha_4(J)$
$\frac{3}{2}$	−0.25 (2)	0.25 (2)		
$\frac{5}{2}$	−0.45 (1)	0.42 (1)	+0.07 (8)	0.08 (9)
$\frac{7}{2}$	−0.67 (4)	0.61 (4)	+0.17 (2)	0.17 (2)
$\frac{9}{2}$	−0.70 (4)	0.64 (4)	+0.26 (10)	0.24 (9)

[a] The errors assigned are $t \cdot (s \cdot d)/\sqrt{n}$, where t is used at the 95% confidence limit.

C. Doppler shift measurements

In reactions where the projectile is light, as in the case of protons, the recoil velocities of the nuclei are small ($\beta = 10^{-2}$ in the present cases) and the corresponding Doppler shifts are small (see Fig. 2). In order to obtain accurate results for the centroid positions of the γ-rays, spectra from the various reactions were accumulated simultaneously with the spectra of radioactive sources chosen so as not to interfere with the measured γ rays.

The theoretical Doppler shift attenuation curves $F(\tau)$ have been calculated as described elsewhere.[8,13] For the calculation of the stopping power the expression

$$T_t = f_e T_e + f_n T_n \qquad (5)$$

was used, where T_t is the total stopping power, e and n refer to electronic and nuclear stopping powers given by the theory of Lindhard *et al.*[14] and f_e and f_n are adjustable parameters. In the present cases the recoil velocity of the residual

TABLE VI. Experimentally measured statistical tensor $\rho_k(J)$ for low lying states in ^{69}Ga, ^{67}Ga, ^{63}Cu, and ^{57}Co as a function of energy.[a]

E_p (MeV)	$\rho_2(\frac{3}{2})$	$\rho_2(\frac{5}{2})$	$\rho_2(\frac{7}{2})$	$\rho_4(\frac{7}{2})$	$\rho_2(\frac{9}{2})$	$\rho_4(\frac{9}{2})$
2.0	−0.18 (4)	−0.43 (2)	−0.64 (6)	0.14 (4)	−0.67 (6)	
2.9	−0.24 (2)	−0.45 (1)	−0.68 (4)	0.18 (2)	−0.70 (4)	0.22 (14)
3.0	−0.25 (2)	−0.45 (1)	−0.67 (4)	0.17 (2)	−0.70 (4)	0.26 (10)
3.3	−0.26 (3)	−0.45 (1)	−0.67 (5)	0.19 (2)	−0.68 (4)	0.30 (15)
4.0	−0.25 (2)	−0.46 (1)	−0.67 (4)	0.18 (2)	−0.72 (4)	0.27 (12)

[a] For the case of ^{69}Ga the bombarding energy was 3.6 MeV to avoid opening of the neutron exit channel.

nuclei was set equal to the velocity of the compound nucleus in the lab system. Since targets of a few mg/cm^2 thickness were used in the experiments, the targets were considered to be composed of 10 sections of equal thickness. Final $F(\tau)$ curves were then calculated by assuming that the reaction took place only at the centers of the respective sections, and then averaging over the entire thickness of the target.

Owing to the high energy of the emitted photons, some additional recoil is imparted to the residual nucleus, which corresponds to about 2–4% of the initial recoil energy. In view of the larger uncertainties associated with the stopping power data, the side feeding time, and the use of a thick target, no serious error is expected to result from the omission of this effect.

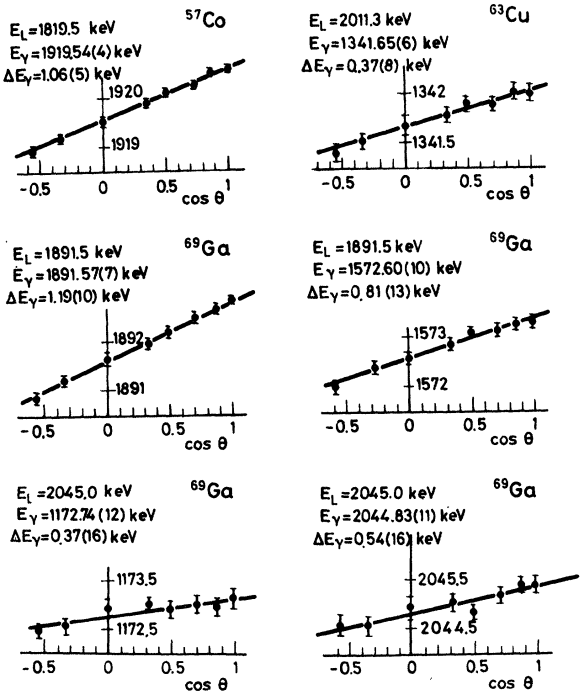

FIG. 2. Examples of measured Doppler shift centroid displacement of some γ rays in ^{57}Co, ^{63}Cu, and ^{69}Ga.

In the present case of the (p,γ) reactions, the low lying ($E^* \leq 2$ MeV) levels of the residual nuclei are fed almost entirely by unobserved γ-ray cascades, originating from the continuum, which are often called "side feeding." The finite mean time of this side feeding contributes to the further attenuation of the observed Doppler shift of the lower lying states.

The $F(\tau)$ curves calculated with $f_e = f_n = 1$ for the ^{56}Fe$(p,\gamma)^{57}$Co and ^{62}Ni$(p,\gamma)^{63}$Cu reactions are very similar and are given in Fig. 3. The corresponding curves for the ^{66,68}Zn$(p,\gamma)^{67,69}$Ga reactions are given in Fig. 4 (curves labeled $\tau_s = 0$). In the same figures the resulting $F(\tau)$ curves, assuming side feeding with different mean lives, are also given.

In all four residual nuclei ^{57}Co, ^{63}Cu, ^{69}Ga, and ^{67}Ga there are states the mean lives of which are reasonably well known either by resonance fluorescence studies or attenuated Doppler shift (see captions of Figs. 3 and 4). These are shown in Figs. 3 and 4 along with their measured $F(\tau)$.

For the case of ^{57}Co and ^{63}Cu all the data lie

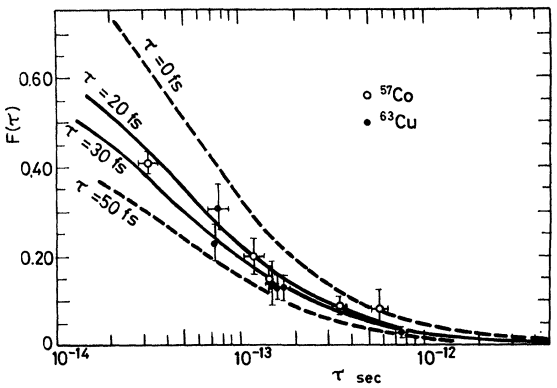

FIG. 3. Calculated $F(\tau)$ curves with different effective side feeding times. The prompt curve correspond to $\tau_s = 0$. For ^{57}Co the mean lives of the 1223, 1896, 1919, 2133, 2523, and 2611 keV states have been obtained from Ref. 15. For ^{63}Cu the mean lives of the 1327, 2011, 1547, 2081, and 2497 keV levels have been obtained from Refs. 9 and 16.

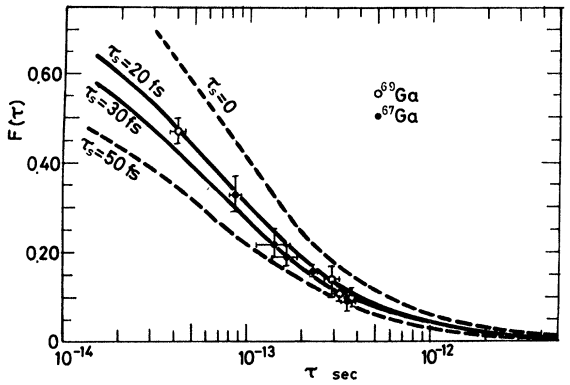

FIG. 4. Calculated $F(\tau)$ curves with different effective side feeding times. For ^{67}Ga the mean lives of the 910, 1554, 1639, 2040, and 2176 keV states are obtained from Refs. 7 and 8. For ^{69}Ga the mean lives of the 872, 1106, 1891, and 2023 keV states are obtained from Refs. 6 and 17.

between the curves which correspond to side feeding times of 20 and 30 fs while for ^{67,69}Ga the data are closer to the curve with $\tau = 20$ fs. Thus the present measurements indicate that the attenuated Doppler shift method can be used for the study of the mean lives of states by assuming a feeding time of the unobserved transition of about 20 fs. The situation here is reminiscent of the case of heavy ion induced reactions. For nuclei in the same mass region it has been found that a side feeding time of ≤ 100 fs can be used to extract mean lives of low lying excited states.[18] In the case of ^{69}Ga discussed in the next section, the attenuation curve with $\tau_s = 20 \pm 5$ fs is used to extract mean lives of excited states in ^{69}Ga.

III. STUDY OF THE EXCITED STATES IN ^{69}Ga

Excited states in ^{69}Ga have been investigated by means of radioactive decay, (^{3}He, d), (d, n), and (d, ^{3}He) (Ref. 19) reactions. The available literature is summarized by Auble.[20] Spin and mixing ratios have been determined for some levels more recently by γ-γ directional correlation studies,[21] and (p, $p'\gamma$) and (n, $n'\gamma$) reactions.[22]

A γ-ray spectrum from the ^{68}Zn(p, γ)^{69}Ga reaction at 3.3 MeV is shown in Fig. 5. In Fig. 6 the decay scheme of ^{69}Ga obtained from the present study is displayed. The new levels introduced at 2007 and 2250 keV have also been observed in the recent (n, $n'\gamma$) reaction.[22] The levels at 2219, 2353, 2458, 2485 and 2529 keV have been observed before either in (^{3}He, d) reactions and/or in (γ, γ') experiments.[20] The level at 2319 keV has been established[23] on the basis of the 1212–1106 keV coincidences observed in the ^{64}Ni(^{7}Li, $2n$) ^{69}Ga reaction. Finally, in the vicinity of 1972 keV, a doublet of levels is established. This doublet has been observed in all particle transfer reactions[20] as an $l = 4$ and $l = 1$ admixture. The 1972 keV member of this doublet decays with the 484 and 636 keV transitions and has been shown previously[20] to be a level with $J^\pi = \frac{9}{2}^+$. The other member of the doublet deexcites with 1973 and 1654 keV transitions to the ground and first excited states in ^{69}Ga. Arnold *et al.*[17] in a resonance fluorescence study of Ga scatterers have confirmed the existence of 1972 and 2007 keV levels deexciting to the ground state, for which they have measured the γ width, but they did not know whether they should assign them to ^{69}Ga or ^{71}Ga. As a result of all these arguments the existence of both 1973 and 2007 keV levels in ^{69}Ga seems quite firm.

In Table VII, the angular distribution of the γ rays deexciting ^{69}Ga as obtained from two separate runs at 3 MeV is shown. For the 1107, 1336, 1487, 1525, 1723, and 1924 keV levels the spin assignments agree with previous experiments.[19-22]

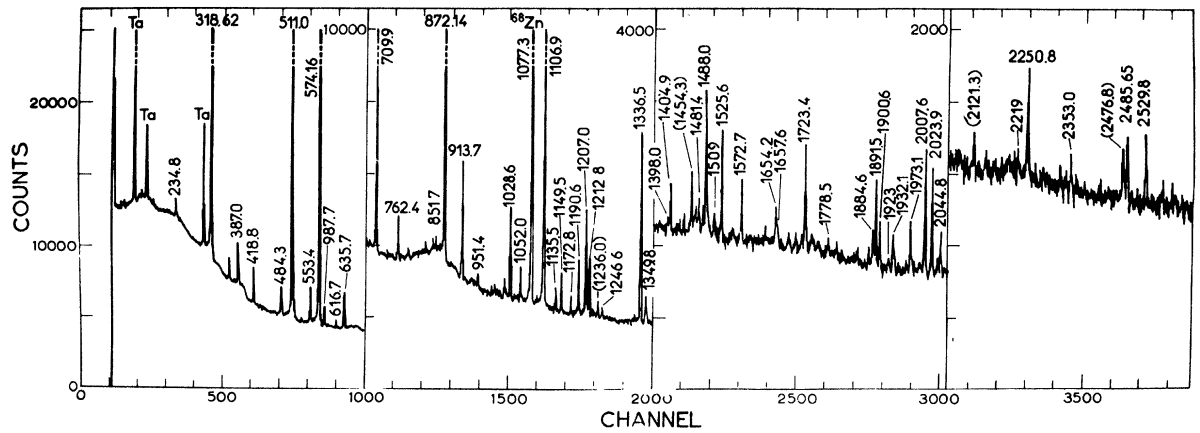

FIG. 5. Gamma-ray spectrum obtained from the ^{68}Zn(p, γ) ^{69}Ga reaction at 3.0 MeV proton energy. Numbers in parentheses are γ rays not placed in the decay scheme.

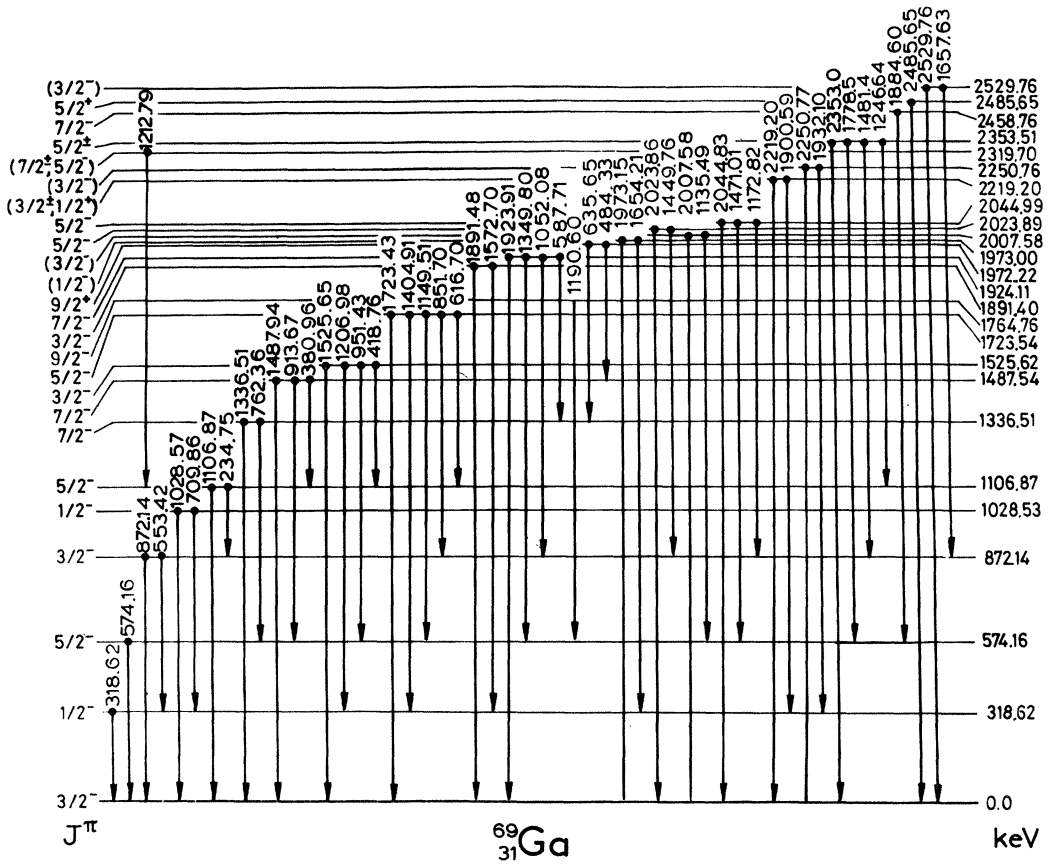

FIG. 6. The resulting decay scheme of ^{69}Ga.

The measured angular distribution allows one to determine the mixing ratio of the transitions deexciting these levels. For the cases where previous measurements are available, the agreement is very good with the currently obtained mixing ratios.

The 1891 keV level has been populated by an $l=1$ transfer in the $(d,{}^3\mathrm{He})$ reaction, and has been assigned $J^\pi=\frac{3}{2}^-$ via (γ,γ') experiments. The measured angular distribution of the γ rays deexciting this level excludes the $\frac{1}{2}$ alternative and allows a firm $\frac{3}{2}^-$ spin assignment. Concerning the 1973 keV level, both of the 1973 and 1654 keV γ rays deexciting it show an almost isotropic distribution and the $\frac{1}{2}^-$ assignment is thus favored.

The γ rays deexciting the 2007 keV level show an angular distribution consistent with $J=\frac{3}{2},\frac{5}{2}$. Kaipov *et al.*[22] in the $(n,n'\gamma)$ reaction reached the same conclusion from the angular distribution of the 2007 keV γ ray alone. This level has been observed with an uncertain $l=1$ transfer in a $^3(\mathrm{He},d)$ reaction and thus it is tentatively assigned $J^\pi=\frac{3}{2}^-$.

The 2024 keV level has been assigned[15] $J^\pi=\frac{5}{2}^-$ or $\frac{7}{2}^-$. The angular distribution of the 2024 keV γ ray excludes the $\frac{7}{2}^-$ assignment.

The 2045 keV level populated in the β decay[20] can have $J^\pi=\frac{7}{2}^-$, $\frac{5}{2}^-$, or $\frac{3}{2}^-$. The angular distribution of the 2045 keV γ ray clearly excludes the $J=\frac{7}{2}^-$ alternative, while the angular distribution of the 1172 keV γ ray excludes the $j=\frac{3}{2}^-$ alternative. Thus a unique $J^\pi=\frac{5}{2}^-$ is made to this level.

For the 2458 and 2485 keV levels, unique spin and parity assignments can be made on the bases of the measured angular distribution and the observed angular momentum transfer in the $(d,{}^3\mathrm{He})$ and $({}^3\mathrm{He},d)$ reactions.[19,20] For the 2353 keV level the angular distribution of the γ rays allows a unique $J=\frac{5}{2}$ assignment while the extracted mixing ratios, although favoring negative parity, do not exclude an opposite parity assignment. For the 2250 and 2529 keV levels a tentative $\frac{3}{2}^-$ spin and parity are proposed.

In Table VIII the average $F(\tau)$ values obtained for the γ rays in ^{69}Ga from all sets of experiments are listed. The deduced mean lives are obtained through the use of the curve of Fig. 4 with $\tau_s=20\pm5$ fs. The statistical error has been added quadratically to the uncertainty arising from the feeding time. For comparison, the mean lives de-

TABLE VII. Angular distribution, branching, and mixing ratios of transitions in ^{69}Ga.

Level (keV)	Transition (keV)	Branch %	J_i (Present)	J_i Others	$J_i \rightarrow J_f$	$A_2 \times 10^2$	$A_4 \times 10^2$	δ Present	δ Others
1106.87 (9)	1106.87 (9)	96.4[a]	$\frac{5}{2}^-$	$\frac{5}{2}^-$[b,c]	$\frac{5}{2}^- \rightarrow \frac{3}{2}^-$	+10.0 (8)	+0.3 (12)	+0.32 (2)	+0.41 (5),[c] +0.34 (4)[d]
1336.51 (6)	762.36 (10)	6.3	$\frac{7}{2}^-$	$\frac{7}{2}^-$[a,b,c]	$\frac{7}{2}^- \rightarrow \frac{5}{2}^-$	+47 (3)	+3 (4)	−2.2 (2)[e]	−2.0 (4)[c]
								or	or
								−0.22 (4)	[−0.68 (10)]
1487.94 (8)	913.67 (7)	36.5	$\frac{7}{2}^-$	$\frac{7}{2}^-$[b,c,d]	$\frac{7}{2}^- \rightarrow \frac{5}{2}^-$	−36 (2)	+8 (2)	−2.85 (30)	−2.54 (10),[c] −3.5 (5)[d]
	380.96 (10)	15.0			$\frac{7}{2}^- \rightarrow \frac{5}{2}^-$	−25 (4)	+2 (4)	−0.03 (3)	
1525.62 (3)	1525.64 (8)	32.0	$\frac{3}{2}^-$	$\frac{3}{2}^-$[a,d]	$\frac{3}{2}^- \rightarrow \frac{3}{2}^-$	−4 (2)	−1 (3)	−0.38 (7)	
	1206.98 (6)	51.0			$\frac{3}{2}^- \rightarrow \frac{1}{2}^-$	−6 (1)	−1 (20)	+0.14 (2)	+0.10 (20)[d]
	951.43 (15)	4.0			$\frac{3}{2}^- \rightarrow \frac{5}{2}^-$	−11 (9)	+10 (13)	+0.3 (3)	
	418.75 (8)	13.0			$\frac{3}{2}^- \rightarrow \frac{5}{2}^-$	−4 (3)	−1 (4)	+0.05 (7)	
1723.54 (10)	1723.43 (13)	42.0	$\frac{5}{2}^-$	$\frac{5}{2}^-$[a,d]	$\frac{5}{2}^- \rightarrow \frac{3}{2}^-$	−51 (4)	+3 (5)	−0.75 (15)	−0.75[d]
	1404.91 (13)	16.0			$\frac{5}{2}^- \rightarrow \frac{1}{2}^-$	+22 (5)	−5 (6)	−0.05 (7)	
	1149.51 (13)	28.0			$\frac{5}{2}^- \rightarrow \frac{5}{2}^-$	−3 (30)	−7 (40)	−0.46 (10)	−0.60 (10)[d]
	851.70 (40)	5.0			$\frac{5}{2}^- \rightarrow \frac{3}{2}^-$				
	616.70 (20)	9.0			$\frac{5}{2}^- \rightarrow \frac{5}{2}^-$	+21 (10)	−6 (13)	+0.05 (25)	
1891.41 (10)	1891.50 (7)	65.0	$\frac{3}{2}^-$	$(\frac{3}{2}^-)$[a]	$\frac{3}{2}^- \rightarrow \frac{3}{2}^-$	+4 (2)	0 (3)	−0.15 (6)	−0.15 (5)[d]
	1572.70 (10)	35.0			$\frac{3}{2}^- \rightarrow \frac{1}{2}^-$	−16 (3)	1 (40)	−0.09 (9)	
1924.11 (10)	1924.20 (50)	9.0	$\frac{7}{2}^-$	$\frac{7}{2}^-$[c,d]	$\frac{7}{2}^- \rightarrow \frac{3}{2}^-$				
	1349.95 (10)	27.0			$\frac{7}{2}^- \rightarrow \frac{5}{2}^-$	−40 (5)	+9 (6)	−2.6 (4)[e]	−2.7 (3),[d] −0.30 (4)[c]
								or	or
								−0.15 (5)	−6.5 (20)
	1052.08 (6)	38.0			$\frac{7}{2}^- \rightarrow \frac{3}{2}^-$	+26 (3)	−6 (4)	$E2$	$E2$[c,d]
	587.71 (6)	23.0			$\frac{7}{2}^- \rightarrow \frac{7}{2}^-$	+29 (3)	−2 (4)	0.00 (7)[e]	−0.03 (7)[c]
								or	or
								+1.1 (1)	−1.0 (1)
1973.0 (15)	1973.15 (10)	67.0	$(\frac{1}{2})^-$		$\frac{1}{2}^- \rightarrow \frac{3}{2}^-$	−2 (3)	+1 (4)		
	1654.21 (15)	33.0			$\frac{1}{2}^- \rightarrow \frac{1}{2}^-$	+1 (6)	+3 (8)		
2007.58 (10)	2007.52 (10)	81.5	$(\frac{3}{2})^-$	$(\frac{3}{2}^-)$[d]	$\frac{3}{2}^- \rightarrow \frac{3}{2}^-$	−16 (2)	+4 (3)	-1.3^{+4}_{-6}	−1.25 (3)[d]
	1135.49 (10)	18.5			$\frac{3}{2}^- \rightarrow \frac{3}{2}^-$	−4 (5)	+3 (6)	−0.38 (9)	
	2007.52		$(\frac{5}{2})^-$		$\frac{5}{2}^- \rightarrow \frac{3}{2}^-$			0.01 (2)	0.00 (5)[d]
	1135.49				$\frac{5}{2}^- \rightarrow \frac{3}{2}^-$			+0.15 (4)	
2023.89 (10)	2023.86(10)	90.0	$\frac{5}{2}^-$	$\frac{5}{2}^-$[d]	$\frac{5}{2}^- \rightarrow \frac{3}{2}^-$	−3 (2)	+2 (3)	+0.16 (3)	+0.15 (5)[d]
	1449.76 (18)	10.0			$\frac{5}{2}^- \rightarrow \frac{5}{2}^-$				
2044.99 (11)	2044.83 (10)	41.0	$\frac{5}{2}^-$	$(\frac{3}{2}^-, \frac{5}{2}^-)$[a]	$\frac{5}{2}^- \rightarrow \frac{3}{2}^-$	6 (7)	+3 (8)	+0.26 (12)	
	1471.01 (10)	34.0			$\frac{5}{2}^- \rightarrow \frac{5}{2}^-$	26 (4)	−5 (5)	+0.17 (14)	
								or	
								−1.15 (25)	
	1172.82 (20)	25.0			$\frac{5}{2}^- \rightarrow \frac{3}{2}^-$	−34 (5)	+3 (7)	−0.23 (5)	
								or	
								−1.8 (2)	

TABLE VII. (*Continued*).

Level (keV)	Transition (keV)	Branch %	J_i (Present)	J_i Others	$J_i \to J_f$	$A_2\times10^2$	$A_4\times10^2$	δ Present	δ Others
2219.20	2218.90 (60)	29.0	$(\frac{3}{2},\frac{1}{2}^+)$	$\frac{1}{2}^+$ [a]	$J-\frac{3}{2}^-$				
	1900.59 (20)	71.0			$J-\frac{1}{2}^-$	−7 (4)	+2 (5)		
2250.76 (15)	2250.77 (15)	67.0	$(\frac{3}{2})^-$	$(\frac{1}{2}^-,\frac{3}{2}^-)$ [a]	$\frac{3}{2}^- \to \frac{3}{2}^-$	+1 (3)	+1 (4)	−0.23 (8)	
	1932.10 (15)	33.0			$\frac{3}{2}^- \to \frac{1}{2}^-$	−11 (5)	2 (6)	+0.03 (12)	
2319.70 (20)	1212.79 (15)	100.0	$(\frac{7}{2}^\pm,\frac{5}{2}^-)$		$\frac{7}{2} \to \frac{5}{2}^-$	−20 (4)	−4 (5)	−0.23 (8)	
					$\frac{5}{2}^- \to \frac{5}{2}^-$			−1.2 (2)	
2353.51 (40)	2353.00 (50)	31.0	$\frac{5}{2}^\pm$		$\frac{5}{2} \to \frac{3}{2}^-$	−20 (13)	8 (15)	−0.04 (30)	
	1778.50 (50)	21.0			$\frac{5}{2} \to \frac{5}{2}^-$				
	1481.40 (50)	27.0			$\frac{5}{2} \to \frac{3}{2}^-$	−31 (2)	3 (14)	−0.19 (20)	
	1246.64 (40)	21.0			$\frac{5}{2} \to \frac{5}{2}^-$	+26 (10)	+8 (12)	+0.17 (30)	
2458.76 (12)	1884.60 (10)	100.0	$\frac{7}{2}^-$	$(\frac{5}{2}^-,\frac{7}{2}^-)$ [b]	$\frac{7}{2}^- \to \frac{5}{2}^-$	−43 (4)	+5 (5)	−0.17 (3)	
2485.65 (10)	2485.65 (10)	100.0	$\frac{5}{2}^+$	$\frac{5}{2}^+$ [a]	$\frac{5}{2}^+ \to \frac{3}{2}^-$	−20 (5)	−3 (6)	−0.04 (6)	
2529.76 (15)	2529.76 (10)	76.0	$(\frac{3}{2})^-$	$(\frac{1}{2}^-,\frac{3}{2}^-)$ [a]	$\frac{3}{2}^- \to \frac{3}{2}^-$	+9 (5)	+4 (6)	−0.03 (10)	
	1657.63 (20)	24.0			$\frac{3}{2}^- \to \frac{3}{2}^-$	+8 (11)	+9 (13)	−0.05 (25)	

[a] Reference 20.
[b] Reference 19.
[c] References 6 and 21.
[d] Reference 22.
[e] Indicates preferred choice.

TABLE VIII. Mean lives of ^{69}Ga levels, obtained by Doppler-shift attenuation method (DSAM) from centroid shift measurements in singles spectra.

Level keV	J^π	γ rays used (keV)	$F(\tau)$	τ (fs)	τ (Ref. 17) Resonance fluorescence (fs)
1525.62	$\frac{3}{2}^-$	1525.6, 1207	0.03 (3)	≥800	≥3500
1723.54	$\frac{5}{2}^-$	1723.3, 1405, 1149	0.02 (1)	≥1400	1300 (450)
1891.41	$\frac{3}{2}^-$	1891.5, 1572.7	0.47 (3)	42 (8)	42 (4)
1924.11	$\frac{7}{2}^-$	1349.8, 1052.0	≤0.05	≥900	≥350
1973.00	$(\frac{1}{2})^-$	1973.0, 1654.2	0.24 (4)	140 (40)	200 (45) if $J=\frac{1}{2}$, 400 (90) if $J=\frac{3}{2}$
2007.6	$(\frac{3}{2})^-$	2007.5, 1135.5	0.08 (3)	510^{+300}_{-150}	490 (70) if $J=\frac{3}{2}$, 730 (102) if $J=\frac{5}{2}$
2023.89	$\frac{5}{2}^-$	2023.9	0.14 (4)	280^{+120}_{70}	290 (30)
2044.92	$\frac{5}{2}^-$	2044.9, 1471.0, 1172.8	0.22 (2)	160 (20)	193 (30)
2219.20	$(\frac{3}{2},\frac{1}{2})$	1900.6	0.07 (5)	≥300	
2250.76	$(\frac{3}{2})^-$	2250.76, 1932.1	0.24 (6)	140^{+70}_{40}	
2319.70	$(\frac{5}{2}^-,\frac{7}{2}^\pm)$	1212.8	≤0.12	≥300	
2353.51	$\frac{5}{2}^\pm$	1481.4, 1246.6	≤0.15	≥250	
2458.76	$\frac{7}{2}^-$	1884.60	0.17 (9)	220^{+280}_{80}	
2485.65	$\frac{5}{2}^+$	2485.65	0.30 (10)	100^{+80}_{40}	
2529.76	$(\frac{3}{2})^-$	2529.8, 1657.6	0.29 (5)	110 (30)	

duced from the γ-ray widths measured by Arnold *et al.*,[17] using the updated branching ratios and spins obtained in the present work, are also shown. The agreement between the two sets of measurements is satisfactory and adds confidence to the method described here.

IV. DISCUSSION

The results presented here demonstrate clearly that useful spectroscopic information can be derived for odd-even nuclei in the mass region $A = 50 - 70$ by the use of semi-thick even-even targets bombarded by protons of low energy.

In this radiative capture process, a large number (500 or more) of states is excited in the compound nucleus, with a virtually complete alignment. These states decay directly or indirectly through a number of intermediate levels to lower lying levels ($E \leq 2.5$ MeV) predominantly by dipole γ transitions. From the measured angular distributions of the γ rays emanating from these lower lying states, it has been concluded that the decay of the highly excited states in the compound nucleus to the lower lying states results in an inevitable but not strong attenuation of the initial alignment.

Moreover, it has been found that the resulting alignment of the lower lying discrete states does not depend significantly on the bombarding energy or the particular residual nucleus, but is characteristic of the spin of the level. All these features may be a result of the statistical nature of the decay of the compound nucleus.

In Fig. 7 the measured attenuation coefficients α_2 and α_4 of the alignment (Table V) are shown as functions of spin. In the same figure, curves are drawn through the points for α_2 and α_4, calculated by assuming Gaussian distributions of the magnetic substates with two different widths, $\sigma = 2.0$ and 1.5 (solid curves in Fig. 7), and a simple exponential distribution. It is clear that none of these assumptions reproduce the observed attenuation of the alignment of the states very well.

Let us try to understand the mechanism of the observed alignment in terms of the attenuation of a statistical nature that would be caused by γ-ray cascading. We thus proceed in the following manner.

(1) We assume that any lower lying level is fed by the states J of the compound nucleus (completely aligned) either directly in a single transition, or through one or more intervening states.

(2) The states formed in the compound nucleus decay by pure dipole transitions to lower lying levels $J-1$, J, and $J+1$.

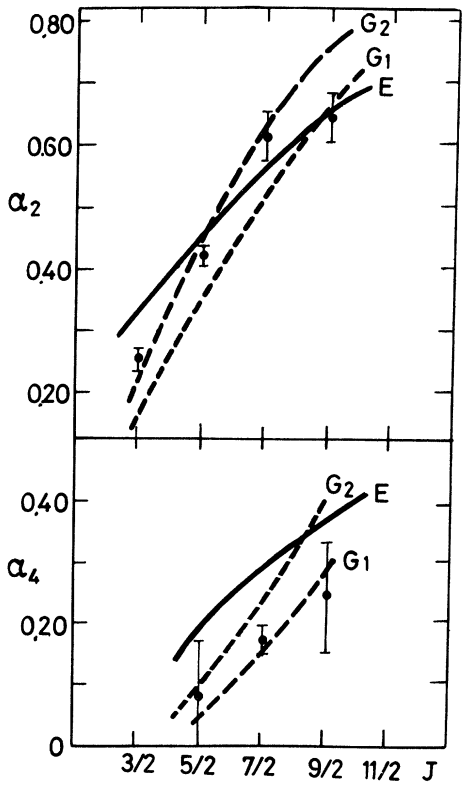

FIG. 7. The α_2 and α_4 attenuation parameters as a function of spin, derived from the present measurements. The curves G_1 and G_2 are drawn through the points calculated with a Gaussian distribution of the magnetic substates with $\sigma = 2$ (curve G_1) and $\sigma = 1.5$ (curve G_2). The curve E is obtained assuming a simple exponential of the form $\exp(-m/\sigma)$ for the distribution of the magnetic substates.

In this way the statistical tensor of a low lying level of spin J_2 fed directly will be

$$\rho_\nu^1(J_2) = \sum_i n^0(i)\rho_\nu^0(i)U_\nu \quad (J_2,\ i,\ L=1), \tag{6}$$

where i runs from $J_2 - 1$ to $J_2 + 1$, $n^0(i)$ is the relative population of the states with $i = J$ excited in the reaction, $\rho_\nu^0(i)$ is the statistical tensor for complete alignment, and U_ν is the well known[5] coefficient which describes the attenuation of the alignment due to a preceding unobserved transition.

For states fed via one intermediate level, an equation similar to Eq. (6) will hold with the upper indices 1 and 0 augmented by one unit, etc. The assumption of pure dipole multipolarities is not so critical in the calculation of the corresponding U coefficients. It can be shown easily that effects arising from possible admixtures of higher order multipoles with $|\delta| \leq 0.25$ can be neglected. The relative populations $n^0(i)$ in Eq. (6) have been calculated through the use of the program CINDY[24]

TABLE IX. Calculated and experimental values of the statistical tensor $\rho_\nu(J_2)$ for the state J_2 fed by unobserved direct (1-step) or cascade γ transitions and undergoing observed γ decay.

Number of γ-cascade transitions between J_1 and J_2	$J_2=\frac{3}{2}$	$J_2=\frac{5}{2}$		$J_2=\frac{7}{2}$		$J_2=\frac{9}{2}$	
	$\rho_{2,i}$	$\rho_{2,i}$	$\rho_{4,i}$	$\rho_{2,i}$	$\rho_{4,i}$	$\rho_{2,i}$	$\rho_{4,i}$
1-step ($i=1$)	−0.2689	−0.7338	−0.0420	−0.9330	0.5302	−1.0041	0.7523
2-step ($i=2$)	−0.1574	−0.3370	0.0102	−0.6508	−0.0071	−0.8662	0.4058
3-step ($i=3$)	−0.0745	−0.1734	−0.0007	−0.3122	0.0079	−0.6240	0.0293
4-step ($i=4$)	−0.0379	−0.0861	0.0002	−0.1610	−0.0001	−0.3248	0.0090
5-step ($i=5$)						−0.1688	0.0009
Experimental $\rho_{\nu\,\mathrm{exp}}$	−0.25 ± 0.02	−0.45 ± 0.01	0.07 ± 0.08	−0.67 ± 0.04	0.17 ± 0.03	−0.70 ± 0.04	0.26 ± 0.10
Theory $\bar{\rho}_{\nu,i}$ for $i=1$	−0.2689	−0.7338	−0.0420	−0.9330	0.5302	−1.0041	0.7523
$i=2$	−0.2132	−0.5354	−0.0159	−0.7919	0.2616	−0.9352	0.5791
$i=3$	−0.1669	−0.4147	−0.0108	−0.6320	0.1770	−0.8314	0.3958
$i=4$	−0.1347	−0.3326	−0.0081	−0.5143	0.1327	−0.7048	0.2991
$i=5$						−0.5976	0.2395

which permits the evaluation of radiative capture processes, including the effects of other competing reactions, in absolute quantitative terms. For the calculation of $n^1(i)$, $n^2(i)$, etc., the original calculated strengths have been redistributed among the intervening states.

The results of the calculation performed for ^{69}Ga are shown in Table IX. From an inspection of the quoted numbers, it is readily seen that the statistical tensors drop quickly to zero as the number of intervening steps exceeds 4. Comparing with the observed experimental statistical tensors it becomes evident that a large fraction of the feeding of the low lying states must originate from cascades which proceed directly from the states formed in the reaction, in order to account for the observed alignment.

Assuming that the occurrence of two or more intermediate states is equally likely, we obtain the average statistical tensors listed in the second part of Table IX as a function of the number of the intermediate γ-ray cascades. From the listing, it appears that the $J=\frac{3}{2}$ states are fed mostly by direct single step decays, while the $J=\frac{5}{2}$ and $\frac{7}{2}$ states are fed directly as well as indirectly with the intervention of two other levels. Finally, the calculations when repeated for different targets or bombarding energies give similar quantitative results as given in Table IX.

From the analysis of the observed Doppler shift of the γ rays deexciting the low lying levels of the nuclei ^{57}Co, ^{63}Cu, ^{67}Ga, and ^{69}Ga, it is concluded that the γ ray cascading from the compound nucleus levels to these low lying levels could be simulated by assuming an effective feeding time of about 20 fs. Although it is difficult to reproduce this number quantitatively, the fact that this feeding time is nearly the same for all nuclei can be accepted qualitatively as caused by the statistical decay of the compound nucleus.

In applying the method described here to the spectroscopic investigation of even-odd nuclei, it should be stressed that although the alignment parameters and side feeding times remain constant within experimental error, in the mass region investigated, and are expected to remain so for nearby nuclei, their behavior has not been examined in nuclei lying far away in mass.

Our present intention is to study in detail, using this method, several nuclei, such as ^{65}Ga, and the odd Cu isotopes, which are important in the evaluation of nuclear models. In parallel, we believe that an extension of the study of the (p,γ) reaction on heavier or lighter nuclei will prove helpful in understanding the alignment mechanism better.

[1]B. A. Nemashkalo, V. E. Storizhko, V. F. Boldyshev, O. I. Ekhichev. A. P. Klyucharev, and A. I. Popov, Yad. Fiz. 17, 229 (1973) [Sov. J. Nucl. Phys. 17, 117 (1973)].

[2]V. F. Boldyschev, B. A. Nemashkalo and V. E. Strizhko, Yad. Fiz. 14, 609 (1971) [Sov. J. Nucl. Phys. 14, 339 (1972)].

[3]E. Sheldon and D. Van Patter, Rev. Mod. Phys. 38, 143 (1966).

[4]K. S. Krane, R. M. Steffen and R. M. Wheeler, Nucl. Data Tables 11, 351 (1973).

[5]Y. Yamazaki, Nucl. Data Tables A1, 453 (1966).

[6]T. Paradellis and G. Vourvopoulos, Phys. Rev. C 18, 660 (1978).

[7]A. M. Al Naser, A. Behbehani, L. O. Green, C. J. Lister, P. J. Nolan, and J. F. Sharpey-Schafer, J. Phys. G 3, 1383 (1977).
[8]T. Paradellis, Nucl. Phys. A279, 293 (1977).
[9]C. T. Papadopoulos, A. G. Hartas, P. A. Assimakopoulos, G. Andritsopoulos, and N. H. Gangas, Phys. Rev. C 15, 1987 (1977).
[10]R. Dayras, B. Cujec, and I. M. Szoghy, Nucl.Phys. A257, 118 (1976).
[11]K. L. Coop, I. G. Graham, and E. W. Tritterton, Nucl. Phys. A149, 463 (1970).
[12]R. Dayras, M. Toulemonde, B. Cujec, B. Hensch, J. N. Mo, and I. M. Szoghy, Nucl. Phys. A173, 49 (1971).
[13]T. Paradellis, I. Galanakis, and G. Vourvopoulos, Nucl. Phys. A307, 472, (1978).
[14]L. Lindhard, M. Scharff, and H. E. Schiøtt, K. Dan. Vidensk. Selsk, Mat.—Fys. Medd. 33, No. 14 (1963).
[15]R. L. Auble, Nucl. Data Sheets 20, 327 (1977).
[16]R. L. Auble, Nucl. Data Sheets 14, 119 (1975).
[17]R. Arnold, E. Booth, and W. Alston, Phys. Rev. C 7, 1490 (1973).
[18]N. Bendjaballah, B. Delaunay, J. Delaunay, and T. Nomura, Nucl. Phys. A280, 228 (1977).
[19]G. Rotbard, G. LaRana, M. Vergnes, G. Berrier, and J. Kalifa, Phys. Rev. C 18, 86 (1978).
[20]R. L. Auble, Nucl. Data Sheets 17, 193 (1976),
[21]T. Paradellis, A. Xenoulis, and C. A. Kalfas, Z. Phys. A 275, 269 (1975).
[22]D. Kaipov, Y. Kosyak, S. Arynov, and I. Shukalov, Yad. Fiz. 30, 1198 (1979) [Sov. J. Nucl. Phys. 30, 623 (1979)].
[23]P. Bakoyeorgos, P. Assimakopoulos, and T. Paradellis (unpublished).
[24]E. Sheldon and V. C. Rogers, Comput. Phys. Commun. 6, 99 (1973).